CONF-9606115--9

SAND95-1151C
SAND--95-1151C

TESTING THE DISTURBED ZONE AROUND A RIGID INCLUSION IN SALT[1]

M.Kathryn Knowles, David Borns, Joanne Fredrich, David Holcomb,
Ronald Price, David Zeuch
Sandia National Laboratories, Albuquerque, NM[2]

Timothy Dale, R. Scott Van Pelt
INTERA, Inc., Austin, TX

ABSTRACT

Deformational processes within a zone of rock surrounding excavations in salt result in alteration of the geophysical and hydrologic properties as compared to the undisturbed condition. The disturbed rock zone offers little resistance to fluid flow. It is hypothesized that rigid inclusions such as concrete seals will arrest and subsequently reverse the disturbance process and induce healing in the disturbed rock. This experiment gathered in situ data that substantiates this hypothesis. A series of tests was conducted in a volume of rock surrounding concrete seals that were emplaced in a 1-m borehole approximately eight years ago. Fluid flow measurements, measurements of geophysical parameters of the surrounding rock, and petrographic analyses on core samples were performed to characterize the rock. This paper presents the testing methodology and summarizes the data gathered from the field test program.

1.0 INTRODUCTION

One of the advantages of placing radioactive waste in natural salt deposits is that the salt undergoes time-dependent deformation, or creep, which will eventually close the repository rooms and encapsulate the waste. The Waste Isolation Pilot Plant (WIPP), a planned disposal site for transuranic wastes, is an underground repository mined from the Salado Formation, which is predominantly halite (i.e., salt). As the continual creep deformation of the salt immediately adjacent to underground openings occurs, conditions for the formation of microfractures become favorable. This process leads to the creation and accumulation of damage in the rock, which gives rise to the disturbed rock zone (DRZ). The work described in the paper is intended to characterize the microscopic DRZ within a salt stratum.

Proposed seal systems for the WIPP recognize DRZ effects and have been designed to acceptably limit the consequences of the enhanced flow potential through the DRZ (DOE, 1995). Long-term sealing functions are fulfilled by columns of reconsolidated salt and compacted bentonite clay emplaced in the WIPP shafts. The

salt members of the sealing system must undergo reconsolidation for several decades to achieve a permeability low enough to acceptably limit fluid flow through the shafts. During this interim, other sealing components, such as concrete, will serve as the principal barriers to fluid flow through the shafts. The existence of a permeable DRZ around seal components may compromise the ability of the seal system to inhibit fluid flow. Geomechanical models of damage resulting from the DRZ and reversal of the damage process predict that the permeability of the DRZ will be reduced as the salt creeps around a rigid seal member such as concrete (Brodsky and Munson, 1994). Although extensive laboratory testing has been conducted in support of model development, no field data exist to evaluate the in situ state of the DRZ around a concrete seal. The test program discussed in this document collected field data on (1) the DRZ resulting from excavation of a seal emplacement borehole and (2) the state of the DRZ in the immediate vicinity of concrete seals emplaced in the borehole approximately eight years prior to this test program. The experimental process and equipment used for the test program are described in Section 2 of this paper. Results from the testing program are presented in Section 3. A brief discussion of the test results and the implications of these results to the WIPP shaft sealing program are presented in Section 4.

2.0 EXPERIMENTAL PROCESS DESCRIPTION AND TEST CONFIGURATION

The tests conducted for this study include fluid flow measurements, geophysical measurements, and petrographic analyses. The rigid inclusions around which the in situ data were taken are two of the concrete seals of the Small Scale Seals Performance Test (Stormont, 1984), which were emplaced in February 1986 in Room D of the WIPP underground experimental area (see Figure 1). The excavation boreholes are approximately 1 m in diameter and 5 m deep. Identical concrete seals, each 1 m in length and 1 m in diameter, were constructed in each borehole at a depth nearly 3 m from the rib of Room D. The seals are located in a stratum comprised of relatively clean halite with small amounts of polyhalite, clay, and anhydrite. A plan view of the borehole layout for all measurements is shown in the enlargement in Figure 1. Test boreholes were drilled around the excavation boreholes to permit both near-field and far-field measurements. Test boreholes located within 0.3 m of the emplacement borehole were considered near-field. Figure 2a is an elevation view of the west rib of Room D showing the locations of all the relevant boreholes. Figure 2b is an isometric view of one excavation borehole showing the sampling locations in the proximal test boreholes.

In general, fluid flow can be directly correlated to formation permeability. Undisturbed halite has extremely low permeability to brine and is essentially impermeable to gas. Existence of gas permeability in salt provides evidence for the existence of desaturated microfractures. Because of uncertainty about the saturation state of the formation, both brine and gas flow tests were conducted. Microfractures in salt result in increased porosity, which produces a decrease in the compressional wave

DISCLAIMER

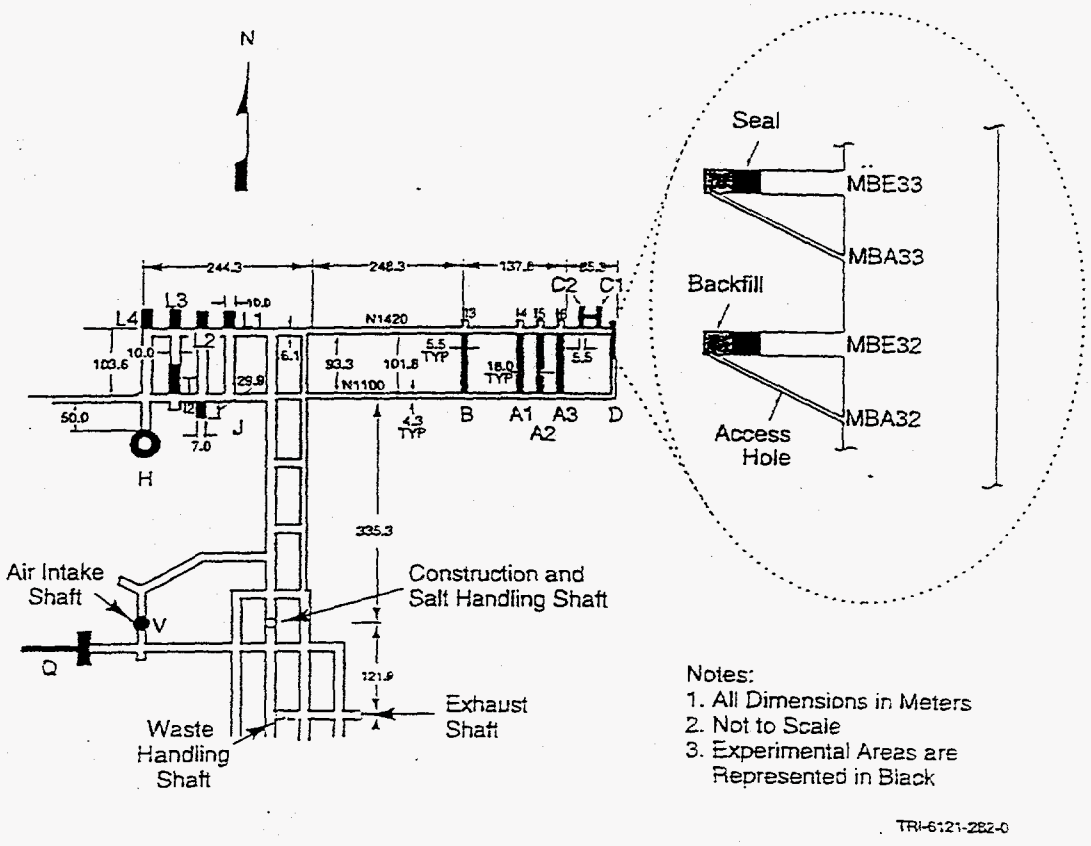

Figure 1. Partial Underground Map of WIPP Experimental Facility. The Enlargement Shows the Configuration of Holes Used for DRZ Testing.

velocity and resistivity of the formation. Measurement of these geophysical parameters can identify the extent of a DRZ. Direct visual observation of the nature and extent of microfractures can be obtained through petrographic studies. Any of these three testing methods can be used to estimate the extent of a DRZ; however, some uncertainty exists for each method. Taken together, results of all testing methods can be used to develop an assessment of the DRZ in the test region.

Fluid Flow Testing

Tests were conducted at various depths in the boreholes to characterize volumes of rock where significant differences of flow potential were expected to exist. Gas-flow testing was conducted using isobutene in instrument grade air as the injection gas and the digital gas flow tool, a pressure control and delivery cabinet that pressurizes and monitors up to four individually inflated packers as well as the interval pressures. A schematic of the test equipment is shown in Figure 3.

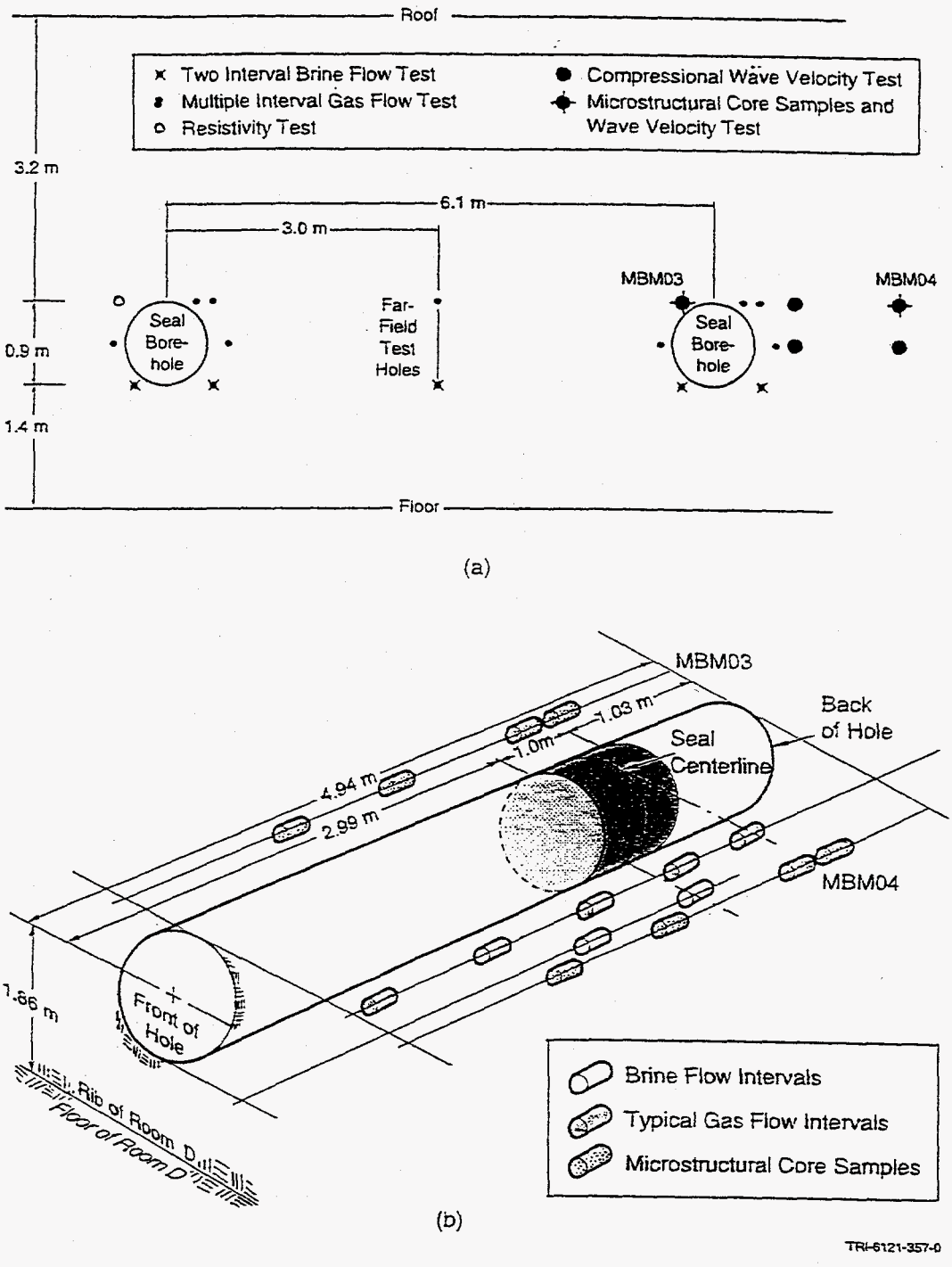

Figure 2. Test Borehole Layout: (a) Elevation Looking West, (b) 3-D View of Excavation Borehole and Test Boreholes.

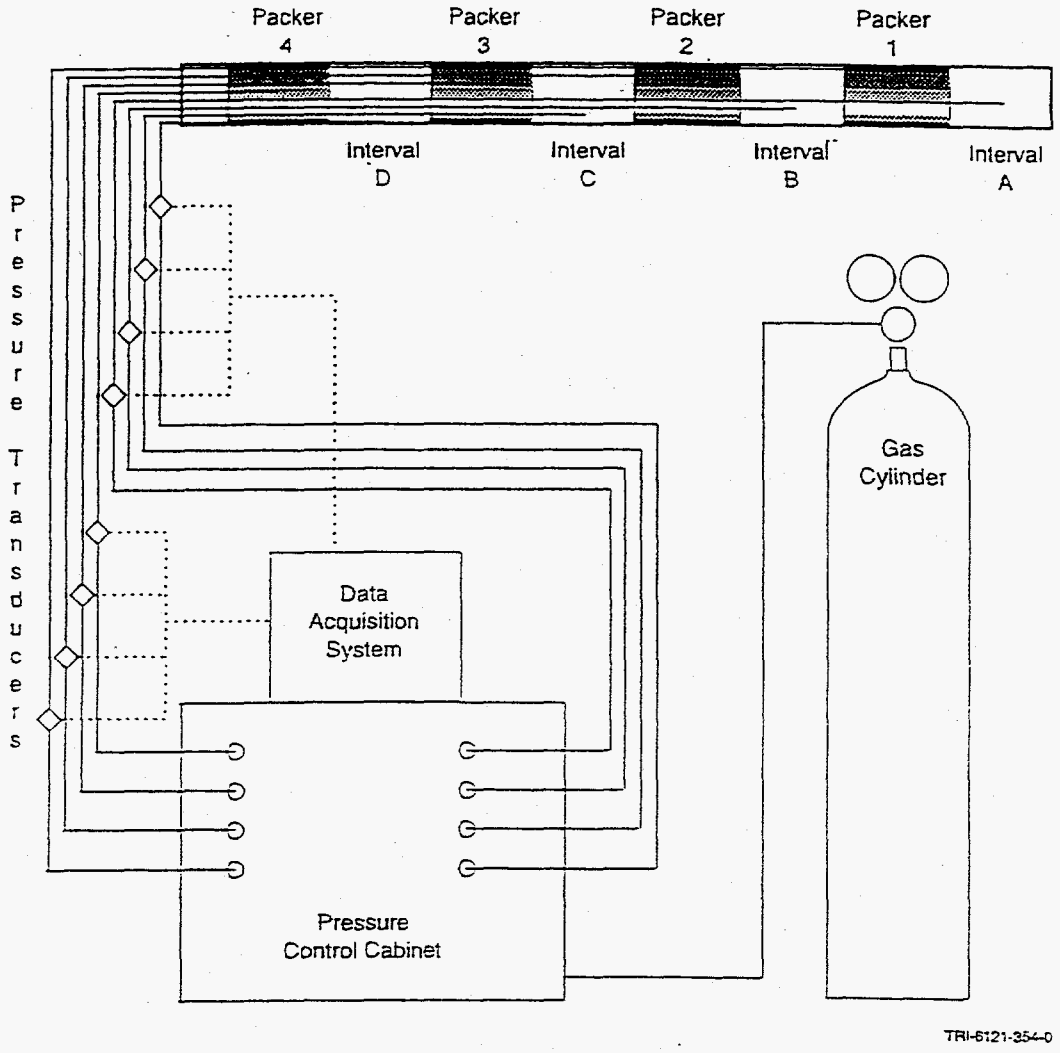

Figure 3. General Test Configuration Schematic for Gas-flow Testing.

Gas-flow testing was performed at four to five depths in nine test boreholes. These boreholes were parallel to and strategically placed with respect to the 1-m diameter seal emplacement boreholes. The far-field test borehole was located at the seal horizontal midline, halfway between the two seal emplacement boreholes. This location allowed 3 m of formation between the test borehole and the seal emplacement borehole.

Three test zones were located at shallower depths (relative to the rib of Room D) than the concrete seal, and one was set at the seal depth. Five boreholes were deepened to allow testing of the zone located behind the concrete seal. Gas-flow testing consisted of a single sequence of a constant-pressure injection test followed by a pressure-decay period. Data files containing time, test-interval pressure, cumulative

gas flow into the test interval, and change in test-zone pressure were collected for each test. These data were subsequently analyzed with the Graph Theory Field Model (GTFM) well-test analysis software (Pickens et al., 1987).

Brine-flow boreholes were drilled to test the interval located at the middle of the 1-m long seal. A two-packer test tool was used for this test component. The lower inflatable packer element was located so that it extended about 0.2 m beyond the uphole edge of the concrete seal. The outer testing interval was located at a depth of about 0.5 m uphole of the concrete seal depth.

Pulse-injection testing was selected in order to test a smaller volume of formation surrounding the test borehole. A pulse-injection test is conducted by increasing the pressure in the designated testing interval to a specified pressure and monitoring the subsequent pressure-decay in the interval. Approximately 24 hours after each borehole was drilled, a packer was installed and testing was initiated. Data were collected and stored for analysis using the GTFM.

Measurement of Geophysical Parameters

Measurements of the host rock compressional wave velocity were taken at near-field and far-field locations (Figure 2). The technique for measuring compressional wave velocity (V_p) is standard (Mattaboni and Schreiber, 1967). An electrical pulse is applied to a piezoelectric transducer, causing an elastic wave to propagate into the material in contact with the transducer. By recording the electrical pulse on an oscilloscope, the origination time of the wave is established and recorded. When the wave reaches the receiver, an identical piezoelectric transducer converts the wave back to an electrical signal that can be recorded on the oscilloscope. From recordings of the wave arrival time and origination time, travel time can be determined. Wave velocity is calculated using the travel time and the path length.

Compressional wave velocity is sensitive to microcracks oriented perpendicular to the wave direction, and microcracks are detectable as a decrease in V_p. The physical extent of the disturbed zone can be determined by propagating waves through successive portions of the salt until an undisturbed zone is reached. Determining the velocity requires an accurate determination of the travel time and the distance between transducers. The propagation distance cannot be measured directly; instead, the transducer insertion depths are measured and used to calculate the propagation distance. Test specifications required an accuracy of 1% for this parameter. Measurements were taken between six hole pairs drilled into the rib of Room D at depth intervals of about 0.3 m. Hole pairs were located in close proximity to the seal emplacement borehole, at distances of 0.5 to 1.0 m from the borehole, and at 1 to 2 m from the borehole.

The electrical resistivity of a rock is related to the rock's porosity, pore saturation and cementation, and the chemical composition of the pore fluid. The increased porosity resulting from microfracturing also produces a change in the net saturation state of the disturbed zone. Resistivity was determined by introducing electrical cur-

rent into the ground through electrodes, then measuring electrical current and electrical potential between other electrodes. Resistivity measurements were taken along the two seal-emplacement boreholes (drilled in 1986), one 0.10-m-diameter access hole (drilled in 1986), and one 0.10-m-diameter test borehole (drilled in 1995).

Petrographic Analysis

Optical microscopy techniques were used to characterize the microcrack damage associated with the DRZ. Core for microstructural investigations (0.10-m diameter) was recovered from two boreholes dry-drilled to depths of 3 to 4 m in proximity to one excavation borehole. Four samples from each core were analyzed, two from a location adjacent to the approximate midpoint of the seal and two from depth intervals corresponding to the open borehole. Subslices were selected from the samples with exactly corresponding depths in both coreholes. Locations of the core subsections were drawn on the cores. The cores were then documented photographically before the eight subslices were sawed and prepared as directionally oriented cubes. Thin and thick petrographic sections were prepared from the oriented cubes. The directional orientation of all specimens was retained.

Prior to initial cutting, the cubes were vacuum-impregnated with a blue-dyed, low-viscosity epoxy to highlight microcracks. A light oil lubricant was used during cutting and polishing to minimize further damage to the rock.

Most petrographic thin sections were examined using an Indus Petroscope. Detailed petrographic observations of thin sections used an Olympus Vanox Universal microscope. Thick sections were examined in ordinary transmitted and reflected light using a Nikon SMZ-10 zoom stereomicroscope equipped with a substage illuminator. Close-up photography and direct visual examination of the thin and thick sections were used to study, record, and analyze fractures. Data were collected using standard stereological techniques (Underwood, 1976).

3.0 EXPERIMENTAL RESULTS

Fluid Flow Testing

Figures 4, 5, and 6 summarize the gas and brine permeabilities for each test borehole. The seal location depth was between 3.0 and 3.8 m into the rib of Room D.

Gas permeability results can be interpreted as a measurement of the intrinsic formation permeability only under fully gas-saturated (i.e., fully desaturated with respect to brine) conditions. The relative gas permeability of halite approaches zero as the brine saturation state approaches unity. The intrinsic permeability of intact halite ranges between 10^{-21} m^2 and 10^{-23} m^2. When the gas permeability approaches that of intact halite, it implies either that the formation in that region is brine saturated or that the formation is undamaged. Correct interpretation of the permeability results will depend on the availability of additional information on damage and saturation.

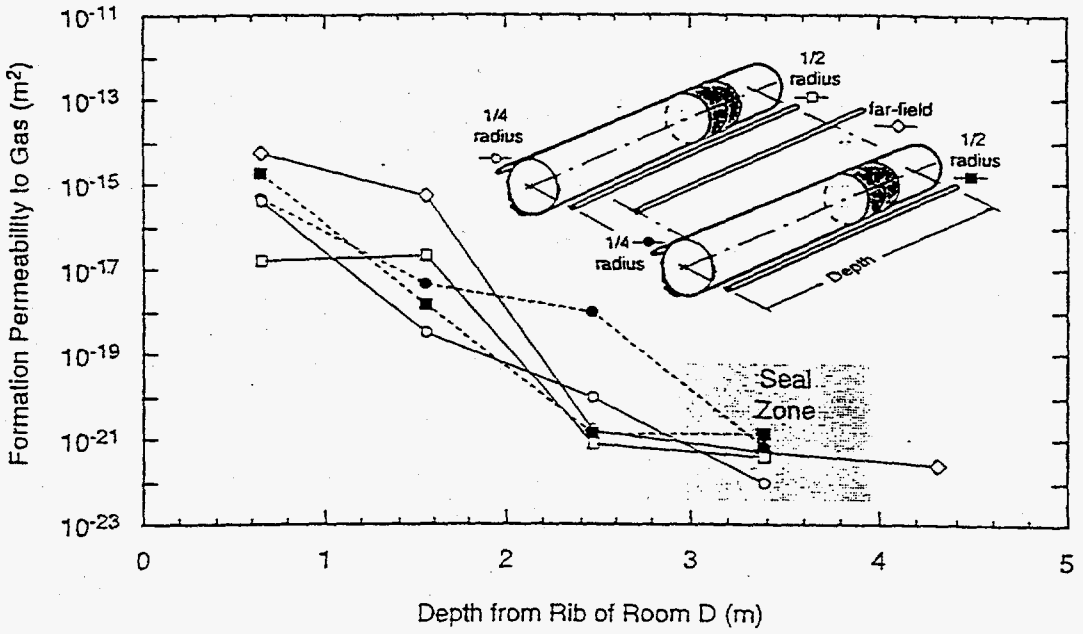

Figure 4. Gas-permeability Estimates for the Far-field and Midline Testing Boreholes as a Function of Depth from the West Rib of Room D.

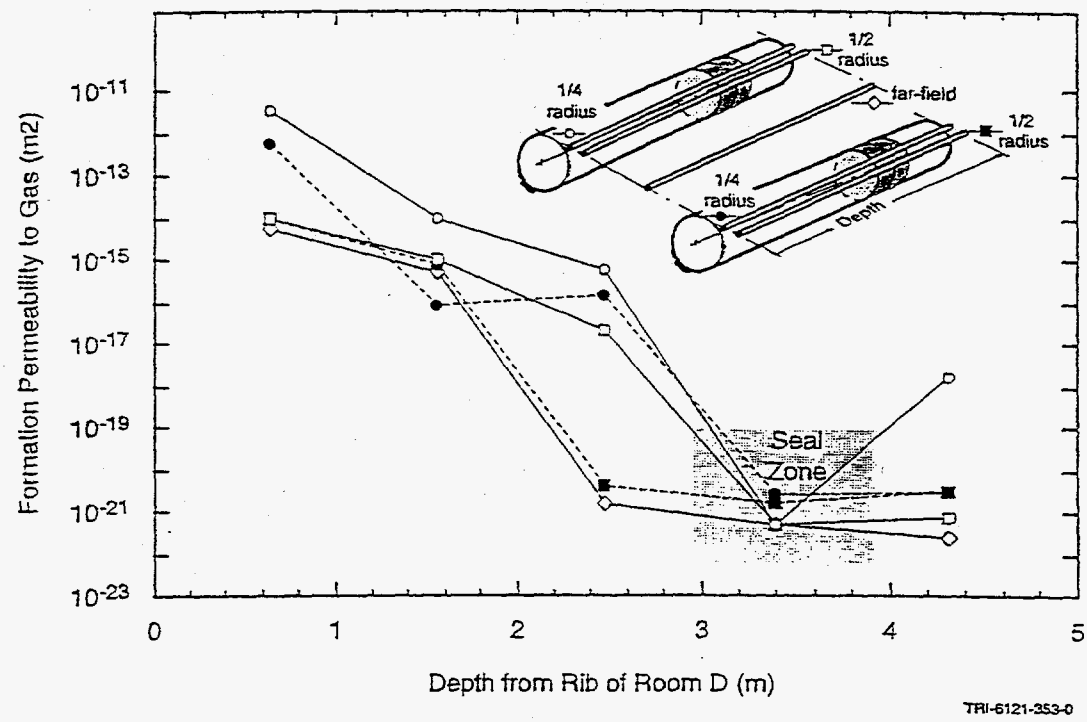

Figure 5. Gas-permeability Estimates for the Far-field and Top Testing Boreholes as a Function of Depth from the West Rib of Room D.

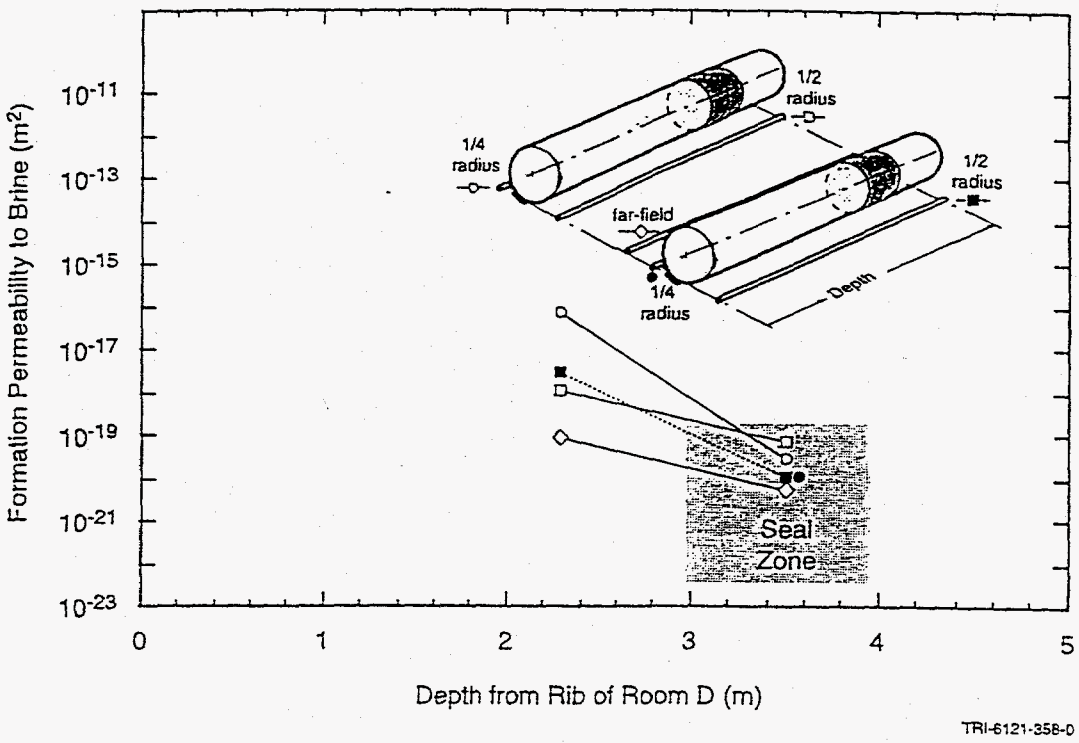

Figure 6. Brine-permeability Estimates for Each Testing Borehole as a Function of Depth from the West Rib of Room D.

Gas flow testing results show that formation permeability to gas (1) decreases as a function of depth from the rib of Room D, (2) decreases as a function of radial distance from the open boreholes, (3) is significantly higher at the top of the borehole than at the midline, and (4) in one case, increases behind the concrete seal. The first and second effects represent reductions in damage as a function of distance from the excavated surfaces of Room D and the emplacement boreholes, respectively. The third effect is best understood in terms of the stress field present in the formation. The emplacement boreholes are not located in the center of the rib of Room D. Stress field calculations conducted using the geomechanical code SPECTROM-32 (Callahan et al., 1990) predict that differential stress at the seal borehole top was significantly greater than differential stress at the seal midline. Because damage in halite is caused by differential stress, the fourth effect is interpreted as a result of circumferential variation in the differential stress around the borehole. Interpretation of the fourth effect requires additional information and will be revisited in Section 4.

Brine-flow testing results are also affected by the saturation state of the formation. The permeability data can be interpreted in a comparative manner. From Figure 4 it is clear that the permeability decreases as a function of distance from the excavated opening. However, effects of the concrete seal cannot readily be determined from these data. The smaller data set for the brine-flow testing limits the conclusions that can be drawn from this test component.

Geophysical Testing

Compressional wave velocities were measured for all six hole pairs. Results for far-field (1 to 2 m from the seal emplacement borehole) and near-field hole pairs are shown in Figures 7 and 8, respectively. Four effects are present in these results. The compressional velocity (1) is a minimum near the rib of Room D, (2) is lower near the open borehole, (3) increases to nearly far-field values at the concrete seal depth, and (4) significantly decreases in the region behind the concrete seal.

The first effect can be attributed to the extensive damage resulting from the presence of Room D. The second effect demonstrates that the stress difference caused by the open borehole increases damage resulting from the DRZ. This damage is eliminated by the rigid seal, as demonstrated by the absence of damage at the seal horizon, and the existence of damage behind the seal. These trends are uniformly consistent with the fluid flow test results.

The resistivity measurements (presented in Figure 9) show a trend similar to that seen in the fluid flow and compressional wave velocity test components, with the additional influence of separation cracks in the emplacement borehole. Cracks parallel to the rib of Room D and along the borehole axis were documented during surveys taken prior to test initiation. The peaks in resistivity at 1 to 2 m along the axis of the excavation boreholes can be attributed to these cracks. At a distance of approximately 2 m from the rib of Room D, all resistivity measurements show an upward trend. The slope of the resistivity curve shows an additional increase at the depth of the concrete seal. No resistivity measurements were taken behind the seal.

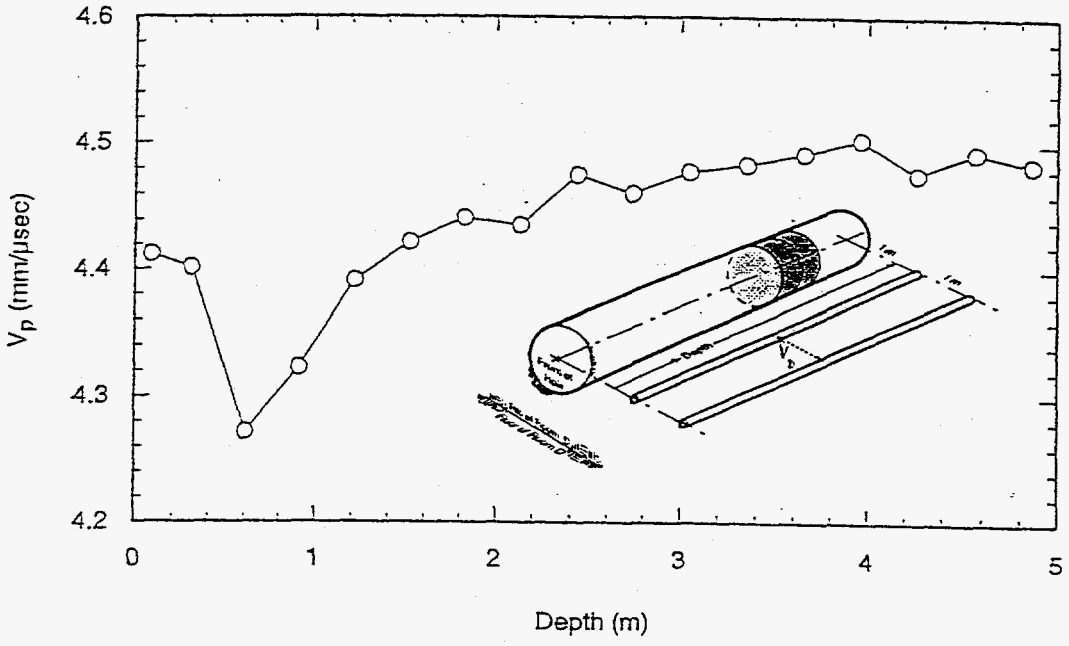

Figure 7. Velocity of Compressional Waves between Far-field Boreholes. Distance between Test Boreholes was 1 m.

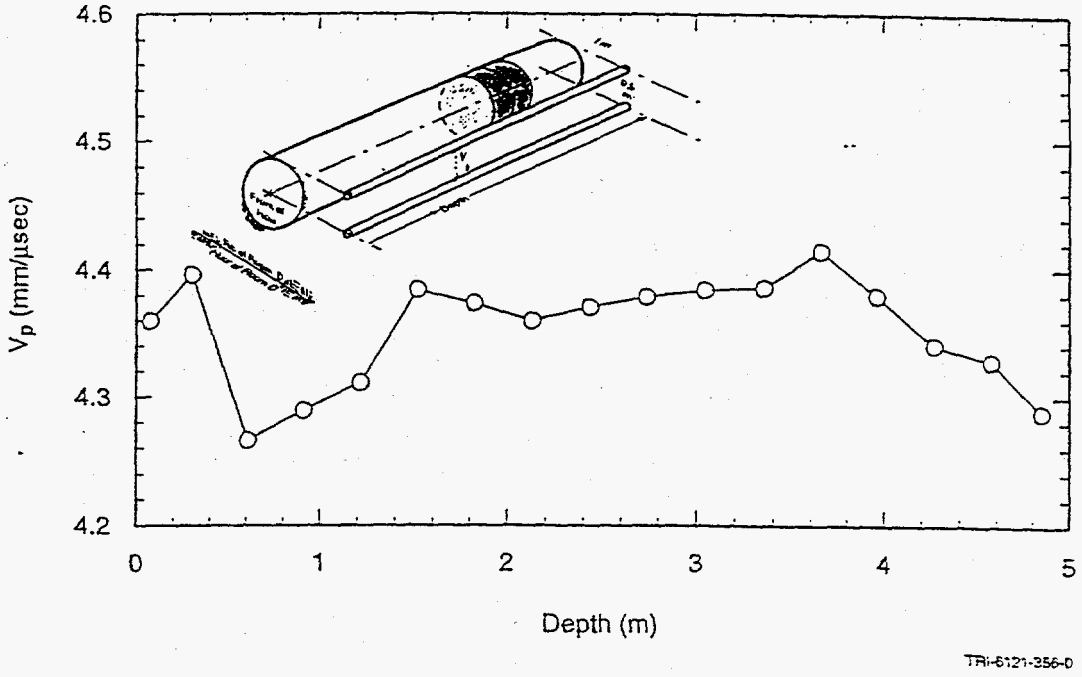

Figure 8. Velocity of Compressional Waves between Near-field Boreholes. Distance between Test Boreholes was 0.5 m.

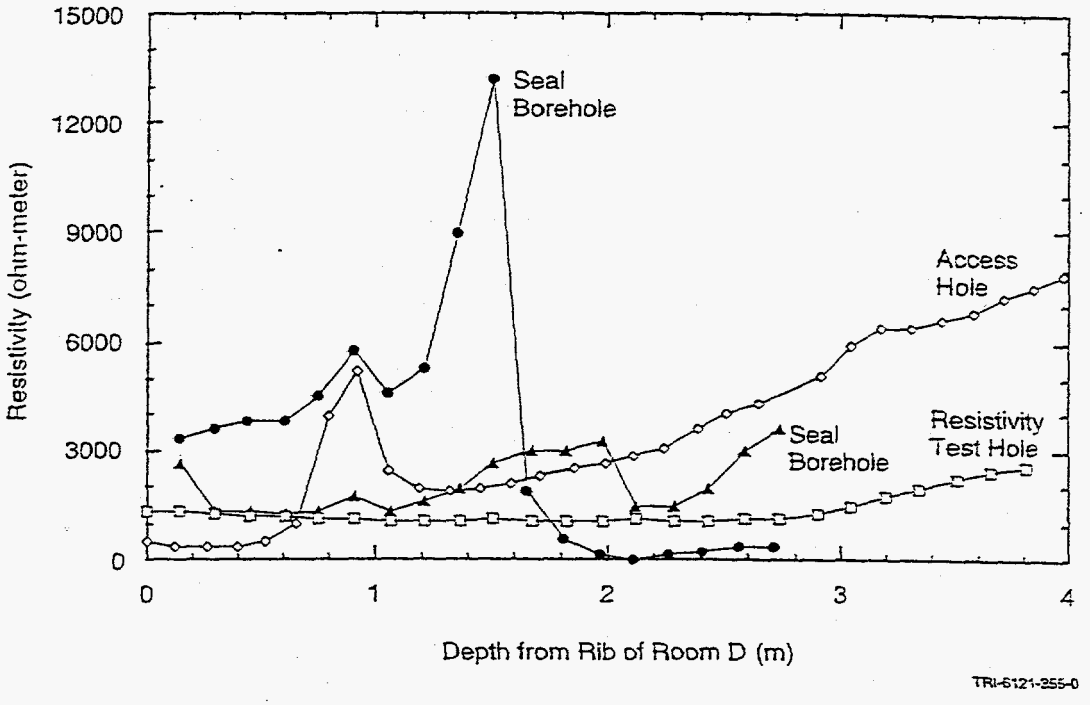

Figure 9. Resistivity Data for Seal Emplacement Boreholes and Test Boreholes.

Petrographic Analysis

The dominant feature of the DRZ in the petrographic sections was found to be dilation along grain boundaries resulting in a network of microcracks (Figure 10). The microcracks were preferentially oriented parallel to the excavation surface of Room D. Damage resulting from the seal borehole should produce cracking parallel to the borehole axis, which is perpendicular to the orientation of D microcracks because of Room D effects. Samples taken near the open borehole showed additional dilation, but there was no change in the orientation of microcracks. All specimens located within a damaged zone exhibited microcracking. However, the crack apertures became much smaller as a function of distance from the excavation surfaces of Room D and the open borehole. Far-field specimens at depths greater than 3 m into the rib of Room D and those in close proximity to the concrete seal exhibited little evidence of damage. The observed damage corresponds directly to increasing formation permeability in the fluid-flow testing and to decreasing compressional wave velocity and resistivity. The absence of damage at the concrete seal horizon suggests that the seal reversed healing of the damage in the surrounding rock.

4.0 DISCUSSION OF RESULTS

A comparative analysis of all data shows that the effects of the Room D DRZ begin to taper off within 2 m into the rib of Room D but remain to a depth of at least 3 m. Damage induced by the open seal borehole can, however, be distinguished from that of Room D. In particular, the fluid flow data show an increased permeability near open boreholes. The single measurement behind one of the concrete seals demonstrates that the formation is damaged at this location. The lower permeability behind the other concrete seal coincides with a zone of low V_p. As discussed in Section 3.0, low gas permeability does not necessarily imply that the rock is undamaged. The low V_p at this location demonstrates that the rock is damaged, but may be partially brine-saturated. Permeability results at far-field test holes all show that intact permeabilities should be expected at depths greater than approximately 3 m. Far-field flow measurements, the measurement of high permeability behind one seal, and low V_p behind the other confirm that the open borehole induces a DRZ that is distinct from the Room D DRZ.

The borehole-induced damage should be observable as microcracks oriented perpendicular to the borehole axis. Although measurements of V_p confirm that these microcracks exist, they were not observed in the petrographic studies. The cracking resulting from the Room D DRZ may have masked these cracks, or the number of pertrographic samples may have been insufficient.

Previous studies have shown that damage occurs immediately upon excavation of an opening (Stormont et al., 1991; Van Sambeek et al., 1993). All experimental data taken in the immediate vicinity of the concrete seal demonstrate that the formation is undamaged in this region. Therefore, it can be concluded that the rigid seal induced reversal of damage. Although some uncertainties exist in the various test components, the consistency of the data support this conclusion. The objectives of the

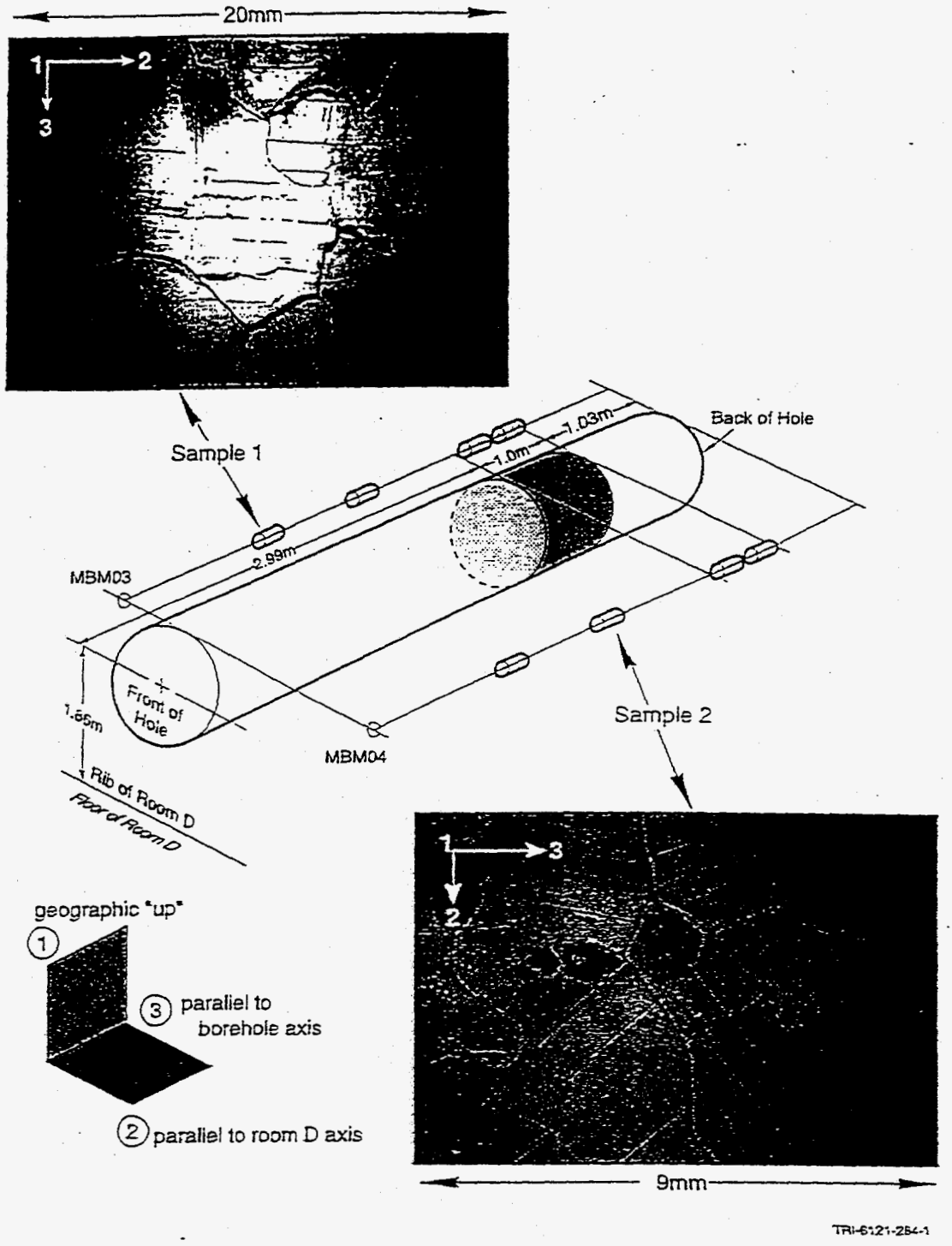

Figure 10. Approximate Sample Locations of Microstructural Studies, Showing Relative Orientation of Axes Marked on Photos of Petrographic Sections Showing Grain Boundary Fractures between Halite Grains.

test program were to collect data relevant to the DRZ surrounding the open borehole and to assess the DRZ in proximity to a rigid inclusion. These objectives were met, and the conclusions support model predictions regarding reversal of damage resulting from the formation of a disturbed zone in salt.

5.0 REFERENCES

Brodsky, N.S., and D.E. Munson. 1994. "Thermomechanical Damage Recovery Parameters for Rocksalt from the WIPP," *Rock Mechanics: Models and Measurements, Challenges from Industry, Proceedings of the 1st North American Rock Mechanics Symposium*, The University of Texas at Austin, Austin, TX. June 1-3, 1994. Eds. P.P. Nelson and S.E. Laubach, Brookfield, VT: A.A. Balkema, 731-740.

Callahan, G.D., A.F. Fossum, and D.K. Svalstad. 1990. *Documentation of SPECTROM-32: A Finite Element Thermomechanical Stress Analysis Program*. DOE/CH/10378-2. RSI-0269. Rapid City, SD: RE/SPEC, Inc.

DOE. 1995. *Waste Isolation Pilot Plant Sealing Systems Design Report*. DOE/WIPP-95-3117. 20 October 1995. Carlsbad NM: US Department of Energy, Waste Isolation Pilot Plant.

Mattaboni, P., and E. Schreiber. 1967. "Method of Pulse Transmission Measurements for Determining Sound Velocities," *Journal of Geophysical Research*. Vol. 72, no. 20, 5160-5163.

Pickens, J.F., G.E. Grisak, J.D. Avis, D.W. Belanger, and M. Thury. 1987. "Analysis and Interpretation of Borehole Hydraulic Tests in Deep Boreholes: Principles, Model Development, and Applications," *Water Resources Research*. Vol. 23, no. 7, 1341-1375.

Stormont, J.C. 1984. *Plugging and Sealing Program for the Waste Isolation Pilot Plant (WIPP)*. SAND84-1057. Albuquerque, NM: Sandia National Laboratories.

Stormont, J.C., C.L. Howard, and J.J.K. Daemen. 1991. *In Situ Measurements of Rock Salt Permeability Change Due to Nearby Excavation*. SAND90-3134. Albuquerque, NM: Sandia National Laboratories.

Underwood, E.E. 1976. *Quantitative Stereology*. Reading, MA: Addison-Wesley.

Van Sambeek, L.L., D.D. Luo, M.S. Lin, W. Ostrowski, and D. Oyenuga. 1993. *Seal Design Alternatives Study*. SAND92-7340. Albuquerque, NM: Sandia National Laboratories.

NOTES

1. This work was supported by the United States DEpartment of Energy under Contract DE-AC04-94AL85000.
Sandia is a multiprogram laboratory operated by Sandia Corporation, a Lockheed Martin Company, for the United States Department of Energy.